

Structure and dynamics of C₆₀ and C₇₀ from tight-binding molecular dynamics

C. Z. Wang, C. T. Chan, and K. M. Ho

Ames Laboratory, Iowa State University, Ames, Iowa 50011

and Department of Physics and Astronomy, Iowa State University, Ames, Iowa 50011

(Received 13 January 1992; revised manuscript received 6 April 1992)

Structural and vibrational properties of C₆₀ and C₇₀ fullerenes are studied by molecular dynamics using a recently developed tight-binding potential model. It is shown that this tight-binding molecular-dynamics scheme has accuracy comparable to *ab initio* techniques and is very efficient for studying the finite temperature properties of fullerenes.

I. INTRODUCTION

The breakthrough in synthesis¹ of C₆₀ and other fullerenes created a very active research area in physics and chemistry. With the success in producing macroscopic quantities of C₆₀ and C₇₀, experimentalists have been able to use nuclear magnetic resonance (NMR) to clarify the structure of these two molecules as having I_h and D_{5h} point-group symmetries, respectively,^{2,3} confirming the predictions made several years ago by Kroto *et al.*^{4,5} At the same time, other experimental techniques such as infrared absorption and Raman and neutron scattering⁶⁻⁸ have also been widely applied to investigate the dynamical properties of these prototype fullerenes.

On the theoretical side, the structural and dynamical properties of the fullerenes have been calculated extensively by various techniques. Most of the calculations are performed at zero temperature except for molecular-dynamics (MD) simulations using the Car-Parrinello method performed by Zhang, Yi, and Bernholc⁹ and by Feuston *et al.*¹⁰ Nevertheless, due to the heavy computational cost, Car-Parrinello simulations have been limited to very short simulation time and many dynamical properties which require longer simulation time have not been well characterized.

Recently, we have undertaken molecular-dynamics simulation studies of the structures and dynamics of the fullerenes using a tight-binding potential model developed in our group. We find that the tight-binding molecular-dynamics (TBMD) scheme, though simple, is very efficient and accurate for use in the study of various properties of the fullerenes. In this paper, we report on the calculations of the structural and vibrational properties of C₆₀ and C₇₀ at both zero and finite temperatures. Comparisons with other theoretical calculations and experimental data are also discussed.

II. TIGHT-BINDING MOLECULAR-DYNAMICS SCHEME

Newton's equations of motion for atoms involved in tight-binding molecular dynamics are derived from a Hamiltonian with the form

$$H(\{\mathbf{r}_i\}) = \sum_i \frac{\mathbf{P}_i^2}{2m} + \sum_n^{\text{occupied}} \langle \psi_n | H_{\text{TB}}(\{\mathbf{r}_i\}) | \psi_n \rangle + E_{\text{rep}}(\{\mathbf{r}_i\}), \quad (1)$$

where $\{\mathbf{r}_i\}$ denotes the positions of the atoms ($i = 1, 2, \dots, N$) and \mathbf{P}_i stands for the momentum of atom i . The first term in (1) is the kinetic energy of the ions, the second term is the electronic band-structure energy calculated by a parametrized tight-binding Hamiltonian $H_{\text{TB}}(\{\mathbf{r}_i\})$, and the third term is a short-ranged repulsive energy. Electronic degrees of freedom are explicitly involved in the force calculation but are not explicitly involved in the dynamics. The latter feature allows a larger time step to be used in the simulation. The time step used in this study (0.7×10^{-15} s) is about a factor of 10 larger than that used in Car-Parrinello simulations.¹⁰

The tight-binding Hamiltonian $H_{\text{TB}}(\{\mathbf{r}_i\})$ for carbon is constructed using an orthogonal sp^3 basis,

$$H_{\text{TB}}(\{\mathbf{r}_i\}) = \sum_i \sum_{\alpha=s,p} \epsilon_\alpha a_{i\alpha}^\dagger a_{i\alpha} + \sum_{i,j} \sum_{\alpha,\beta=s,p} v_{\alpha,\beta}(r_{ij}) a_{i\alpha}^\dagger a_{j\beta}, \quad (2)$$

where $a_{i,\alpha}$ represents the α orbital on the i th atom, ϵ_s and ϵ_p are the on-site energies of the carbon $2s$ and $2p$ orbitals, and $v_{ss\sigma}(r_{ij})$, $v_{sp\sigma}(r_{ij})$, $v_{pp\sigma}(r_{ij})$, and $v_{pp\pi}(r_{ij})$ are overlap parameters between two orbitals whose centers are separated by distance r_{ij} . The repulsive energy is expressed in the form $E_{\text{rep}} = \sum_i f[\sum_j \phi(r_{ij})]$, where $\phi(r_{ij})$ is a pairwise potential between atoms i and j , and f is a fourth-order polynomial function.

The parameters and scaling functions used in the present calculations are taken from our previous work.¹¹ Such a tight-binding potential model not only reproduces well the binding energies and bond lengths of crystalline carbon phases with different coordination numbers, but also describes well the properties of several complex carbon systems far away from the ground state such as liquid and amorphous carbon. The reliability of the model for applications to carbon clusters is demonstrated by comparing the ground-state geometries obtained by the present tight-binding model with the results of accurate

quantum-mechanical calculations for small clusters. In the range $5 \leq n \leq 11$, we found that odd-numbered clusters prefer a ring structure.¹¹ This result agrees well with the accurate *ab initio* calculations of Raghavachari and Binkley.¹² Since the potential parameters are determined by fitting to the bulk properties, we expect that the potential will become even more reliable as the cluster size gets bigger.

III. GROUND-STATE PROPERTIES

The tight-binding potential model discussed in Sec. II is first used to calculate the ground-state properties of C_{60} and C_{70} . The geometries of the fullerenes are optimized by simulated annealing using the tight-binding molecular-dynamics scheme. The initial configurations used for the structural optimization are distorted C_{60} spheroid-shaped and C_{70} ellipsoid-shaped cages with the atoms in the correct topological framework but with distorted bond angles and bond lengths. We heat the molecules up to 500 K and gradually cool them down to 0 K without any constraint. This optimization process leads to ideal fullerene structures for C_{60} and C_{70} as shown in Fig. 1. The C_{60} molecule is a truncated icosahedron (I_h point-group symmetry) in which all atoms have the same environment. The carbon-carbon bond lengths are 1.396 Å for the “double bonds” (the shared hexagon edges) and 1.458 Å for the “single bonds” (the pentagon edges), respectively. These values are in very good agreement with experimental data^{13–15} and *ab initio* calculation results^{9,10,16} (see Table I). The symmetry of the C_{70} molecule is D_{5h} . This molecule contains five types of non-equivalent atoms (as labeled *a–e* in Fig. 1) with the ratio $a:b:c:d:e = 10:10:20:10:10$. There are eight distinct carbon-carbon bond lengths among the five nonequivalent atoms. As one can see from Table II, the bond lengths of C_{70} obtained from our tight-binding calcula-

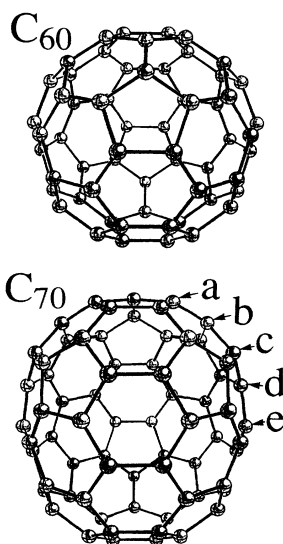


FIG. 1. Perspective views of C_{60} and C_{70} . The letters *a, b, c, d, and e* label the five nonequivalent atoms of C_{70} .

TABLE I. Bond lengths of C_{60} . Present results are compared to local-density approximation (LDA), modified neglect of differential overlap (MNDO), and Hartree-Fock calculation results, and to experimental NMR and neutron-scattering data. All results are given in Å.

| | Double bond | Single bond |
|----------|---------------------------------------|---------------------------------------|
| Present | 1.396 | 1.458 |
| LDA | 1.40, ^a 1.39 ^b | 1.45 ^{a,b} |
| MNDO | 1.40 ^c | 1.474 ^c |
| HF/3-21G | 1.365 ^c | 1.453 ^c |
| NMR | 1.40±0.015 ^d | 1.45±0.015 ^d |
| Neutron | 1.39, ^e 1.391 ^f | 1.46, ^e 1.455 ^f |

^aReference 9.

^bReference 10.

^cReference 16.

^dReference 13.

^eReference 14.

^fReference 15.

tion are also in good agreement with other theoretical calculations^{16,17} and the available experimental data.¹⁸

The vibrational properties of C_{60} and C_{70} at $T=0$ K are studied by solving the eigenvalues and eigenfunctions of a 180×180 (for C_{60}) or a 210×210 (for C_{70}) force constant matrix derived from the Hamiltonian of Eq. (1). The results of the vibrational frequencies are classified according to the symmetry of the I_h and D_{5h} point groups and listed in Tables III and IV, respectively. We found that the 46 distinct vibrational modes of C_{60} are equally divided into even and odd parities. The modes with T_{1u} symmetry are infrared active and those with A_g and H_g symmetries are observable by Raman spectroscopy. As one can see from Table III, the present theoretical results are in good agreement with the available infrared and Raman data,^{6,7} particularly considering that the properties of C_{60} have not been used in the fitting database to determine the tight-binding potential parameters. For C_{70} , the 204 normal modes as listed in Table IV have the following symmetry structure:

$$\Gamma_{D_{5h}} = 12A'_1 + 9A'_2 + 9A''_1 + 10A''_2 + 21E'_1 + 22E'_2 + 19E''_1 + 20E''_2. \quad (3)$$

There are only onefold- and twofold-degenerate vibrational modes. According to the symmetry selection rule, the Raman active modes are those with A'_1 , E'_2 , and E''_1 symmetries and the infrared-active modes are those with A'_2 and E'_1 symmetries. The Raman and infrared spectra of C_{70} have been reported by Bethune *et al.*⁷ However, since so many modes are Raman and infrared active, it is still very difficult to compare the present results with the experimental data without knowing the scattering matrix elements.

IV. FINITE TEMPERATURE PROPERTIES

Using the tight-binding molecular-dynamics scheme, we have investigated the behavior of C_{60} and C_{70} mole-

TABLE II. Bond lengths of C₇₀. Present results are compared to LDA, MNDO, and Hartree-Fock calculation results, and to experimental data. All results are given in Å.

| | Present | LDA ^a | MNDO ^b | HF/3-21G ^b | Expt. ^c |
|--------------------------------|---------|------------------|-------------------|-----------------------|--|
| C _a -C _a | 1.457 | 1.448 | 1.473 | 1.452 | 1.464±0.009 |
| C _a -C _b | 1.397 | 1.393 | 1.402 | 1.370 | 1.37±0.01 |
| C _a -C _c | 1.454 | 1.444 | 1.469 | 1.447 | 1.47±0.01 |
| C _c -C _c | 1.389 | 1.386 | 1.389 | 1.356 | 1.37±0.01 |
| C _c -C _d | 1.456 | 1.442 | 1.478 | 1.458 | 1.46±0.01 |
| C _d -C _d | 1.443 | 1.434 | 1.442 | 1.414 | 1.47 ^{+0.01} _{-0.03} |
| C _d -C _e | 1.418 | 1.415 | 1.430 | 1.403 | 1.39±0.01 |
| C _e -C _e | 1.452 | 1.467 | 1.484 | 1.475 | 1.41 ^{+0.03} _{-0.01} |

^aReference 17.

^bReference 16.

^cReference 18.

cules at finite temperatures. In our simulations, the structural properties are monitored by calculating the radial distribution function $j(r)$ and the angular distribution functions $g_3(\theta)$. $j(r)$ is defined such that $j(r)dr$ gives the average number of atoms whose distance from a given atom is between r and $r+dr$. The $g_3(\theta)$ counts only those angles spanned by bonds with bond lengths less than 1.80 Å. The dynamical properties of the fullerenes at finite temperatures are studied by calculating

the vibration spectra of the fullerenes through Fourier transformation of the velocity-velocity correlation functions using the trajectories generated by the molecular-dynamics simulation. The overall vibrational density of states is given by

$$I(\omega) = \sum_{n=1}^N \int_0^{\infty} dt e^{i\omega t} \langle \mathbf{v}_n(t) \cdot \mathbf{v}_n(0) \rangle, \quad (4)$$

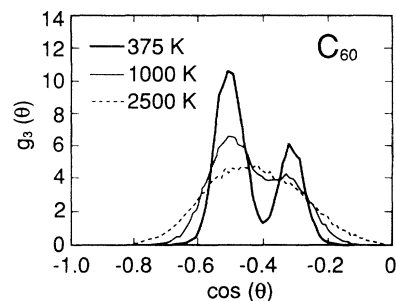
where N is the total number of atoms in the molecule.

TABLE III. Vibration frequencies of the C₆₀ molecule. The numbers inside the parentheses next to the I_h group representation labels indicate the degeneracies of the corresponding group representations. Experimental Raman and infrared data from Ref. 7 are also listed (values inside the parentheses next to the calculated frequencies) for the purpose of comparison.

| I_h label (even parity) | Frequency (cm ⁻¹) | I_h label (odd parity) | Frequency (cm ⁻¹) |
|------------------------------|--|-----------------------------|--|
| $A_g(1)$ | 1610(1470) 509(496) | $A_u(1)$ | 968 |
| $T_{1g}(3)$ | 1293 823 551 | $T_{1u}(3)$ | 1573(1428) 1201(1183) 602(577) 485(527) |
| $T_{3g}(3)$ | 1369 880 800 520 | $T_{3u}(3)$ | 1619 1197 1027 694 327 |
| $G_g(4)$ | 1585 1321 1100 807 549 454 | $G_u(4)$ | 1524 1338 955 875 752 318 |
| $H_g(5)$ | 1653(1575) 1538(1428) 1273(1250) 1135(1099) 786(774) 690(710) 392(437) 237(273) | $H_u(5)$ | 1642 1357 1230 768 633 516 360 |

TABLE IV. Vibration frequencies of C_{70} in units of cm^{-1} .

| A'_1 | A'_2 | A''_1 | A''_2 | E'_1 | E'_2 | E''_1 | E''_2 |
|--------|--------|---------|---------|--------|--------|---------|---------|
| 232 | 460 | 301 | 307 | 297 | 201 | 224 | 288 |
| 366 | 524 | 509 | 420 | 329 | 279 | 369 | 343 |
| 469 | 632 | 581 | 590 | 385 | 410 | 445 | 371 |
| 533 | 752 | 774 | 686 | 479 | 474 | 486 | 498 |
| 688 | 904 | 816 | 946 | 547 | 501 | 525 | 528 |
| 716 | 957 | 904 | 1159 | 558 | 638 | 654 | 612 |
| 1115 | 1243 | 1248 | 1233 | 620 | 679 | 728 | 699 |
| 1246 | 1349 | 1361 | 1438 | 661 | 745 | 755 | 736 |
| 1248 | 1497 | 1630 | 1591 | 780 | 764 | 800 | 792 |
| 1551 | | 1659 | | 830 | 787 | 822 | 872 |
| 1601 | | | | 892 | 832 | 1059 | 939 |
| 1659 | | | | 906 | 884 | 1180 | 1107 |
| | | | | 1124 | 973 | 1242 | 1167 |
| | | | | 1203 | 1082 | 1315 | 1268 |
| | | | | 1269 | 1208 | 1334 | 1330 |
| | | | | 1328 | 1282 | 1467 | 1352 |
| | | | | 1352 | 1370 | 1548 | 1508 |
| | | | | 1481 | 1378 | 1596 | 1543 |
| | | | | 1533 | 1460 | 1654 | 1599 |
| | | | | 1572 | 1575 | | 1641 |
| | | | | 1648 | 1596 | | |
| | | | | 1644 | | | |

FIG. 3. Angular distribution functions of C_{60} .

For C_{60} , we also calculate the vibrational spectra for the even- and odd-parity modes separately,

$$I_{\text{even}}(\omega) = \sum_{I=1}^{N/2} \int_0^{\infty} dt e^{i\omega t} \langle [\mathbf{v}_I(t) - \mathbf{v}_{-I}(t)] \cdot [\mathbf{v}_I(0) - \mathbf{v}_{-I}(0)] \rangle, \quad (5)$$

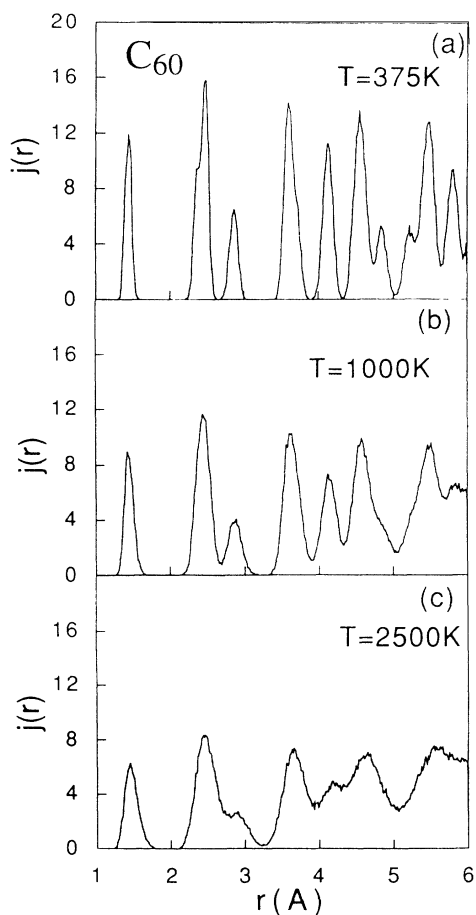
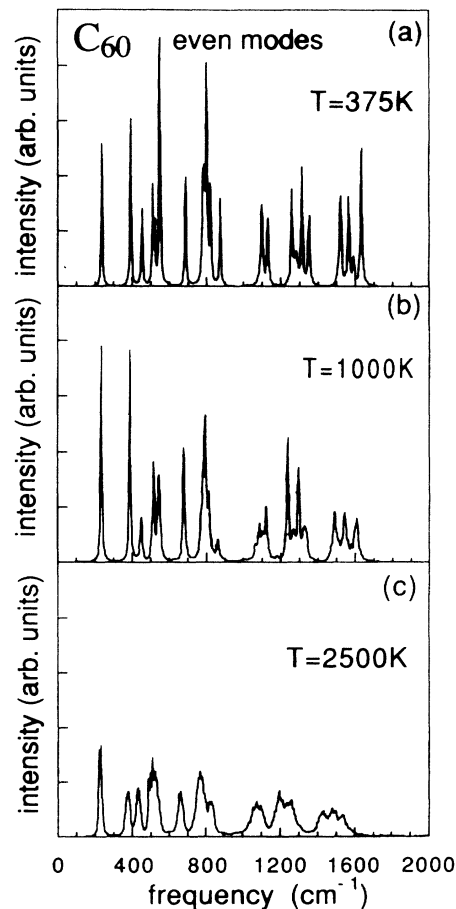
FIG. 2. Radial distribution functions of C_{60} .

FIG. 4. Temperature dependence of the vibrational spectra of the even-parity modes of C_{60} . The spectra have been normalized and broadened by a Gaussian function with a width of 4 cm^{-1} .

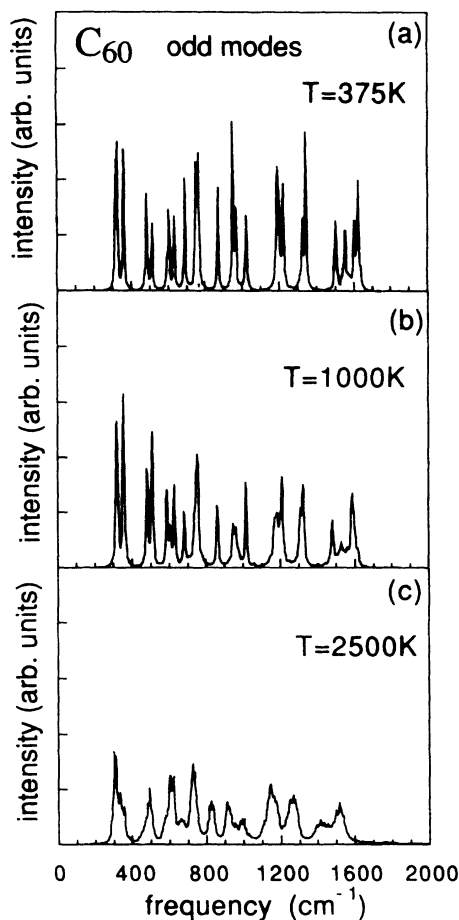


FIG. 5. Temperature dependence of the vibrational spectra of the odd-parity modes of C₆₀. The spectra have been normalized and broadened by a Gaussian function with a width of 4 cm⁻¹.

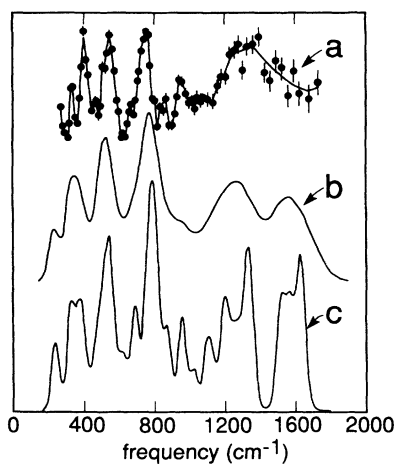


FIG. 6. Vibrational density of states of C₆₀. Upper: Neutron-scattering results (Ref. 8); middle: TBMD results at 375 K broadened by a Gaussian function with experimental instrument resolution quoted from Ref. 8 (low-resolution scan); lower: TBMD result at 375 K broadened by a Gaussian function with width of 30 cm⁻¹.

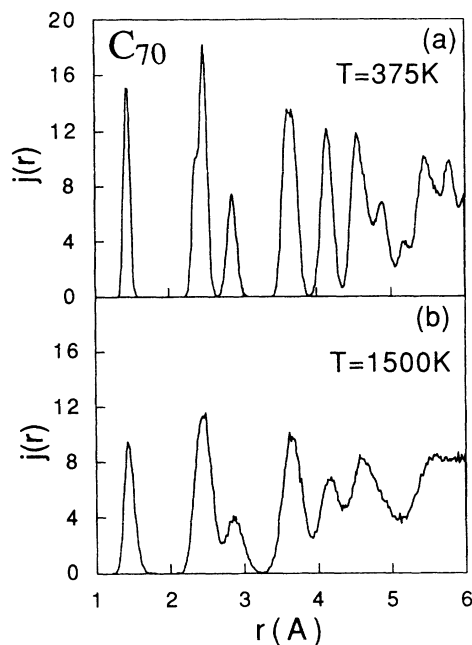


FIG. 7. Radial distribution functions of C₇₀.

$$I_{\text{odd}}(\omega) = \sum_{I=1}^{N/2} \int_0^{\infty} dt e^{i\omega t} \langle [\mathbf{v}_I(t) + \mathbf{v}_{-I}(t)] \cdot [\mathbf{v}_I(0) + \mathbf{v}_{-I}(0)] \rangle, \quad (6)$$

where the subscripts I and $-I$ denote a pair of atoms which are equivalent under inversion in the ideal C₆₀ molecule. At each temperature, 4000 to 6000 MD steps with the temperature control method of Andersen,¹⁹ followed by 2000 MD steps without temperature control are used to thermalize the system. Then the trajectory over an additional 8096 MD steps (corresponding to 6.3 ps) without temperature control is used to perform the statistical average and to calculate the velocity-velocity correlation functions.

The results of radial distribution functions and angular distribution functions of C₆₀ are shown, respectively, in Figs. 2 and 3 for several temperatures ranging from 375 to 2500 K. At 375 K, the peaks in the radial distribution functions are sharp and well defined. The positions of the

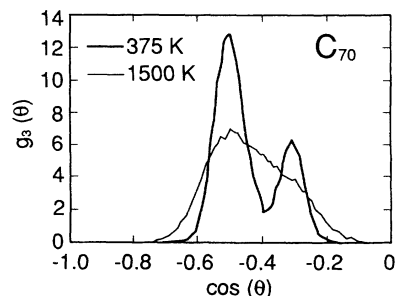


FIG. 8. Angular distribution functions of C₇₀.

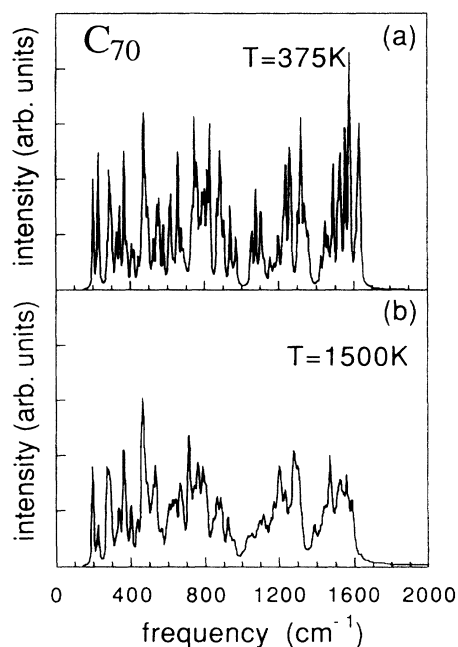


FIG. 9. Temperature dependence of the vibrational spectra of C_{70} . The spectra have been normalized and broadened by a Gaussian function with a width of 4 cm^{-1} .

peaks compare well with the results of *ab initio* molecular-dynamics simulation¹⁰ and neutron diffraction.¹⁴ As the temperature is increased, the peaks become broad but are still distinguishable even at 2500 K. This result is consistent with the strong carbon-carbon bond in the fullerenes. In the angular distribution of Fig. 3, two peaks around 180° and 120° are clearly seen at 375 K. However, these two peaks broaden rapidly with temperature and merge together already at 1000 K. Only a single broad peak is observed at 2500 K.

The vibrational spectra of C_{60} as a function of temperature are shown in Fig. 4 for even-parity modes and in Fig. 5 for odd-parity modes, respectively. At 375 K, the peaks in the spectra are in one-to-one correspondence with the vibration frequencies at 0 K as listed in Table III although some frequencies are slightly shifted due to temperature effects. These peaks broaden and shift towards lower frequencies as the temperature is increased. The frequency shifts of the higher-energy modes are found to be much larger than those of the lower-energy modes.

The vibration spectrum of C_{60} has also been measured recently by neutron-scattering experimentation.⁸ Unlike Raman or infrared, neutron scattering provides the overall vibrational density of states rather than certain selected individual modes. As shown in Fig. 6, we found

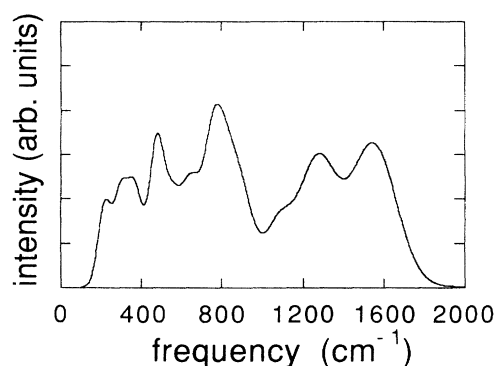


FIG. 10. Vibrational density of states of C_{70} at 375 K. The spectra have been broadened by a Gaussian function with experimental instrument resolution quoted from Ref. 8 (low-resolution scan).

that the overall vibrational density of states obtained by our TBMD scheme at 375 K is in good agreement with the neutron-diffraction data.

In Figs. 7–10, the structural and dynamical properties of C_{70} at finite temperatures are presented. The temperature dependence of these properties is very similar to that of C_{60} . Although the numbers and symmetries of individual vibrational modes of C_{60} and C_{70} are very different (see Table III and IV), their overall vibrational density of states is very similar and will be difficult to distinguish by neutron-diffraction experiments.

V. SUMMARY

In summary, we have demonstrated that tight-binding molecular dynamics is sufficiently accurate and efficient to allow us to perform realistic simulations of fullerenes. The structural and vibrational properties of C_{60} and C_{70} calculated from the present scheme compare well with experimental data and *ab initio* calculations. We anticipate that the scheme will be very useful in the study of more complex processes such as nucleation and reaction as well as fragmentation.

ACKNOWLEDGMENTS

Ames Laboratory is operated for the U.S. Department of Energy by Iowa State University under Contract No. W-7405-ENG-82. This investigation was supported by the Director of Energy Research, Office of Basic Energy Sciences including a grant of computer time on the Cray computers at Lawrence Livermore Laboratory and by NSF under Grant No. DMR-8819379.

¹W. Krätschmer, L. D. Lamb, K. Fostiropoulos, and D. R. Huffman, *Nature (London)* **347**, 354 (1990).

²R. D. Johnson, G. Meijer, and D. S. Bethune, *J. Am. Chem. Soc.* **112**, 8983 (1990).

³R. Taylor, J. P. Hare, A. K. Abdulle-Sada, and H. J. Kroto, *J.*

Chem. Soc. Chem. Commun. **20**, 1423 (1990).

⁴H. W. Kroto, J. R. Heath, S. C. O'Brien, R. F. Curl, and R. E. Smalley, *Nature (London)* **318**, 162 (1985).

⁵H. W. Kroto, *Nature (London)* **329**, 529 (1987).

⁶W. Krätschmer, K. Fostiropoulos, and D. R. Huffman, *Chem.*

- Phys. Lett. **170**, 167 (1990).
- ⁷D. S. Bethune, G. Meijer, W. C. Tang, H. J. Rosen, W. G. Golden, H. Seki, C. A. Brown, and M. S. de Vries, Chem. Phys. Lett. **179**, 181 (1991).
- ⁸R. L. Cappelletti, J. R. D. Copley, W. A. Kamitakahara, F. Li, J. S. Lannin, and D. Ramage, Phys. Rev. Lett. **66**, 3261 (1991).
- ⁹Q. Zhang, J.-Y. Yi, and J. Bernholc, Phys. Rev. Lett. **66**, 2633 (1991).
- ¹⁰B. P. Feuston, W. Andreoni, M. Parrinello, and E. Clementi, Phys. Rev. B **44**, 4056 (1991).
- ¹¹For details of the tight-binding model, see C. H. Xu, C. Z. Wang, C. T. Chan, and K. M. Ho, J. Phys. Condens. Matter **4**, 6047 (1992).
- ¹²K. Raghavachari and J. S. Binkley, J. Chem. Phys. **87**, 2191 (1987).
- ¹³C. S. Yannoni, P. P. Bernier, D. S. Bethune, G. Meijer, and J. R. Salem, J. Am. Chem. Soc. **113**, 3190 (1991).
- ¹⁴F. Li and J. S. Lannin, in *Proceedings of the International Symposium on the Physics and Chemistry of Finite Systems: From Clusters to Crystals*, edited by P. Jena, S. N. Khanna, and B. K. Rao (Kluwer Academic, Boston, 1992).
- ¹⁵W. I. F. David, R. M. Ibberson, J. C. Matthewman, K. Prasad, T. J. S. Dennis, J. P. Hare, H. W. Kroto, R. Taylor, and D. R. M. Walton, Nature (London) **353**, 147 (1991).
- ¹⁶K. Raghavachari and C. M. Rohlfing, J. Chem. Phys. **95**, 5769 (1991).
- ¹⁷W. Andreoni, F. Gygi, and M. Parrinello, Chem. Phys. Lett. **189**, 241 (1992).
- ¹⁸D. R. McKenzie, C. A. Davis, D. J. H. Cockayne, D. A. Muller, and A. M. Vassallo, Nature (London) **355**, 622 (1992).
- ¹⁹H. C. Andersen, J. Chem. Phys. **72**, 2384 (1980).

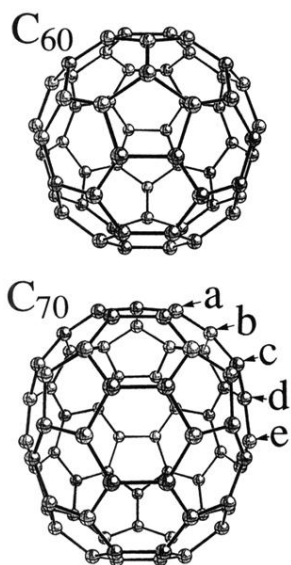


FIG. 1. Perspective views of C_{60} and C_{70} . The letters a , b , c , d , and e label the five nonequivalent atoms of C_{70} .